Earth, Planets and Space

FULL PAPER

Open Access

Global characteristics of the westward-propagating quasi-16-day wave with zonal wavenumber 1 and the connection with the 2012/2013 SSW revealed by ERA-Interim

Wei Li[1], Chunming Huang[1,2,3*] and Shaodong Zhang[1,2,3]

Abstract

We analyze global characteristics of the westward-propagating quasi-16-day wave (Q16DW) with zonal wavenumber 1 (W1) in the troposphere and stratosphere using zonal wind, meridional wind, vertical velocity, temperature, geopotential, and potential vorticity data from the European Centre for Medium-Range Weather Forecasts (ECMWF) Interim Re-Analysis during one year from December 2012 to November 2013. The amplitudes of the W1 Q16DW are larger in the stratosphere than in the troposphere, and remarkable amplitudes are found at middle and high latitudes in the Northern Hemisphere (NH). More detailed analyses on the temporal variation in the W1 Q16DW show that this wave is significantly enhanced during the 2012/2013 Stratospheric Sudden Warming (SSW) event, and the strong wave most likely provides additional forcing on the splitting of the displaced polar vortex. Analysis of the Eliassen–Palm flux (EP flux) and its divergence of the interaction between W1 Q16DW and quasi-stationary planetary waves with wavenumber 1 during the 2012/2013 SSW event reveals that it causes an upward heat flux and exerts a westward acceleration on the background winds, indicating that this interaction plays an important role in the eastward stratospheric jet reversal. Moreover, the wave is amplified in the occurrence region of barotropic and/or baroclinic instability, suggesting a local source of the growing W1 Q16DW during this SSW event.

Keywords: Quasi-16-day wave, Stratosphere, SSW

Introduction

Atmospheric planetary waves (PWs) are global-scale waves that play a key role in the transport of energy, momentum and chemical species, both vertically and horizontally. Most PWs originate in the troposphere, propagate upward, and then break in the middle atmosphere, leading to coupling between the lower and middle atmosphere. PWs can be divided into quasi-stationary and traveling planetary waves. The dynamic processes underlying the two kinds of PWs are generally quite different (Charney and Drazin 1961; Andrews et al. 1987; Vincent 1990; Dunkerton 1991). Quasi-stationary PWs, whose constant-phase surfaces are fixed with respect to the Earth, are generally generated in the troposphere due to topography and diabatic heating. Traveling PWs, whose phase surfaces move, are excited by an irregular thermal or mechanical forcing in the lower atmosphere and instabilities in the middle atmosphere. Traveling PWs with periods near 2, 5, 10, and 16 days in the actual atmosphere have been widely reported during the past several decades (Salby 1984; Wu et al. 1993, 1994; Forbes

*Correspondence: huangcm@whu.edu.cn
[1] School of Electronic Information, Wuhan University, Wuhan, Hubei, China
Full list of author information is available at the end of the article

and Zhang 2015; Huang et al. 2017; Forbes et al. 1995; Day et al. 2011).

Previous studies have mainly focused on the classical normal mode. For frequently observed westward-propagating disturbances with a period of about 16 days, Madden (1978) first identified them with the second symmetric normal mode, i.e., (1, 3) mode and named them the 16-day wave. The normal modes appear in the upper stratosphere and mesosphere as global structures in the equinoctial season and localized ones within the winter hemisphere in the solstitial season (Salby 1984; Hirooka and Hirota 1985). Andrews et al. (1987) concluded that the wave amplitude of this mode is roughly equatorially symmetric at equinoxes and is much larger in the winter hemisphere than in the summer hemisphere at solstices. However, during the winter season, the traveling PW activity is strong and there exist many traveling wave components which are not identified as normal mode waves. Daley and Williamson (1985) found that the 16-day wave in January 1979 is not the manifestation of the theoretical normal modes. Therefore, the normal mode of the quasi-16-day waves is not the only wave with a period near 16 days. The quasi-16-day wave components are more complex in the actual atmosphere. Hereafter, we use Q16DW as the abbreviation for the "quasi-16-day wave", which refers to global-scale waves with a period of nearly 16 days, and they may have different zonal wavenumbers. From recent observational research, McDonald et al. (2011) indicated that the westward- and eastward-propagating Q16DWs with zonal wavenumbers 1 and 2 are generally dominant. They also found that the westward- and eastward-propagating waves with zonal wavenumber 1 have similar magnitudes and are strong in the Northern Hemisphere (NH), while eastward-propagating waves with zonal wavenumbers 1 and 2 are larger than other modes in the Southern Hemisphere (SH). Although all of the modes can affect the atmospheric dynamical structure, the westward-propagating mode with zonal wavenumber 1 (W1 mode) is still the most studied mode. Pervious work showed that the W1 mode plays a key role in the modulation of the various stratospheric phenomena in the NH (Day et al. 2011; Pancheva et al. 2008).

Charney and Drazin (1961) indicated that the effective index of refraction for PWs in the atmosphere depends primarily on the variation of the mean zonal wind with height. They also concluded that the escape of large amounts of planetary wave energy is prevented by the westward or large eastward zonal wind above the tropopause. Although their conclusions are drawn from quasi-stationary PWs considerations, they are still applicable for traveling PWs. Using temperature data from Microwave Limb Sounder on Aura satellite observations, Day et al. (2011) showed that the Q16DW has large amplitudes in regions of strong eastward flow in the stratosphere. Luo et al. (2002) indicated that the Q16DW can penetrate into the weak westward flow. Previous studies of the Q16DW amplitudes have reported a clear seasonal cycle in the mesosphere and lower thermosphere (Mitchell et al. 1999; Luo et al. 2002; Day and Mitchell 2010; Day et al. 2011). They found that the Q16DW amplitude maximum generally occurs around wintertime, while a secondary maximum with a comparatively smaller value is sometimes observed in summertime. Only a few studies on the seasonal cycle of the Q16DW in the troposphere and stratosphere have been reported. These analyses are limited to a single physical quantity and specific latitude and height range. Using temperature data from satellite instruments, Alexander and Shepherd (2010) exhibited the distribution and variability in the Q16DW in the lower to middle stratosphere (15–40 km) of the Arctic (60 °N–70 °N) and Antarctic (60 °S–70 °S). They found that the Q16DW had larger amplitudes in the Arctic winter than in the Antarctic winter. However, there is still a lack of relevant studies about the global characteristics of the Q16DW. ECMWF Interim Re-Analysis (ERA-Interim) data, which can provide relatively complete physical quantities, such as horizontal wind and temperature data from ground to stratosphere, are very useful for showing more comprehensive results of the Q16DWs on a global scale.

Stratospheric Sudden Warming (SSW) is the clearest and strongest manifestation of the stratosphere-troposphere system coupling, which often takes place at high latitudes in the NH wintertime (Charlton and Polvani 2007). SSW events involve dramatic reversals of the temperature gradient, zonal-mean winds and meridional circulation (Andrews et al. 1987). The mechanism for SSW, initially proposed by Matsuno (1971) and now widely accepted, is related to the growth of upward-propagating PWs from the troposphere into the stratosphere and their interaction with the zonal-mean flow. The interaction decelerates sometimes even reverses the eastward winter stratospheric winds. Garcia (1987) indicated that PWs associated with SSW drive a meridional circulation, inducing a downward circulation and adiabatic heating near the pole in the stratosphere. During SSW events, the breakup of stratospheric Arctic polar vortex is affected mostly by strong PW activity. It has been well established that the Arctic polar vortex can be identified with the evolution of the potential vorticity (PV) and geopotential height, and the vortex itself will be strongly displaced or split during a major SSW event (Charlton and Polvani 2007; Matthewman et al. 2009). The major SSW events are typically classified into two types: displacement events, in which quasi-stationary PWs with a

zonal wavenumber of 1 (SPW1) play a primary role, and split events, in which quasi-stationary PWs with a zonal wavenumber of 2 (SPW2) play a major role (Charlton and Polvani 2007; Coy et al. 2009; Bancalá et al. 2012; Chandran and Collins 2014; Butler et al. 2017). In addition, there is another type of complex major SSW event that is rarely analyzed. This event cannot be absolutely defined as the SPW1 or SPW2 pattern (Manney et al. 2005; Kuttippurath and Nikulin 2012), since the polar vortex first displaces from the pole and then splits into two or more vortices. How, or if, the traveling PWs affect the polar vortex is an open question.

The period preceding SSW events is usually characterized by high PW activity in the stratosphere, during which more than one type of PW may exist. The role of quasi-stationary PWs in the generation of SSW events has been well understood and quantified in previous studies (Lin 1982; Scott and Polvani 2006; Pogoreltsev 2007; Iida et al. 2014). However, it is only recently that the relationship between traveling PWs and SSW events has attracted significant attention (Gu et al. 2016; Pancheva et al. 2018; Matthias et al. 2012). In particular, recent studies have shown that the presence of the Q16DW has an important influence on the dynamics of the SSW. Pancheva et al. (2008) concluded that the enhanced traveling PW activity around periods of ~16 days plays an important role in the coupling of the stratosphere–mesosphere system during the major 2003/2004 SSW event. During the SSW events of 2003/2004, 2005/2006 and 2007/2008, Vineeth et al. (2010) found that the enhanced Q16DW and zero wind line propagate simultaneously from the equator to the pole. Xiong et al. (2018) indicated that SPW2 is modulated by the Q16DW and plays a key role in energy transmission during the 2016/2017 SSW event. Using wind data from meteor radars to analyze the Q16DW during the 2013 SSW event, Chen et al. (2016) revealed that this wave is amplified at 86–95 km and enhanced the coupling of the ionosphere and the lower atmosphere during high solar activity. Although these results mentioned above may indicate that the Q16DW changes throughout the atmosphere are associated with SSW events in the NH, the exact role of the Q16DW in the occurrence of SSW events is still unclear. Therefore, in this paper, we investigate the contribution of the Q16DW to the zonal-mean flow and polar vortex in detail during the 2012/2013 SSW event. We also provide insight into the sources of the wave in this case.

The rest of this paper is structured as follows. The next section gives a brief description of the data and analytical methods. The global characteristics of the W1 Q16DW are exhibited in the third section. In the fourth section, we present an overview of the 2012/2013 SSW event and discuss the role of the W1 Q16DW during this major SSW event. The propagation and origins of the W1 Q16DW in the winter of 2012/2013 are also described. A summary is given in the fifth section.

Data and method of analysis

Data from ERA-Interim are used throughout this study. The ERA-Interim reanalysis provides three-dimensional profiles of physical parameters with a time resolution of 6 h from 1979 to the present (Dee et al. 2011). In this study, the data are distributed in a horizontal grid of $2.5° \times 2.5°$ (longitude × latitude) at 37 vertical pressure levels extending from 1000 to 1 hPa. Compared with other reanalysis projects produced by ECMWF, ERA-Interim solves more data assimilation problems and improves accuracy by using a 4-dimensional variational data assimilation system with a 12-h analysis window and ECMWF Integrated Forecasting System model.

As one of the latest global atmospheric reanalysis datasets, ERA-Interim is widely used to study global-scale waves, e.g., Kelvin waves, PWs, and tides (Flannaghan and Fueglistaler 2011; Seppälä et al. 2013; Lu et al. 2012; Sakazaki et al. 2012), and mesoscale gravity waves (Schroeder et al. 2009). It is also used to study quasi-biennial oscillation and SSW (Gómez-Escolar et al. 2014; Škerlak et al. 2014; Iza and Calvo 2015). From the perspective of the temporal and spatial resolutions and height coverage, the ERA-Interim data are quite suitable for studying PWs in the troposphere and stratosphere, especially their global distribution and seasonal variation.

It is well known that the background atmosphere is very important for the propagation and dissipation of atmospheric waves. In our study, the zonal-mean zonal wind, meridional wind, and temperature are taken as the background atmosphere, and those in January 2013 are shown in Fig. 1. In general, there is an eastward wind in the troposphere in both hemispheres, with maximums of 44.4 ms^{-1} in the NH at 175 hPa and 34.0 ms^{-1} in the SH at 250 hPa. In the stratosphere, the eastward wind is still active in middle latitudes of the NH, and the strongest wind is 40.3 ms^{-1} at 45 °N and 1 hPa, while a westward wind is present in the SH and in low latitudes of the NH. The strongest westward wind is 81.0 ms^{-1} at 15 °S and 1 hPa. The weak westward wind in the stratosphere in high northern latitudes may be associated with the major SSW in January 2013. Compared with the zonal wind, the meridional wind is quite weak, and its magnitude is between − 4.0 ms^{-1} and 3.5 ms^{-1}. The slightly stronger southward wind takes place in the stratosphere in middle and high latitudes, and the northward wind is present in the equatorial tropopause and stratopause. In January 2013, a stratospheric warming occurs at high latitudes of the NH, with a maximum of 235 K. In the stratosphere, the observed monthly averaged temperature structure

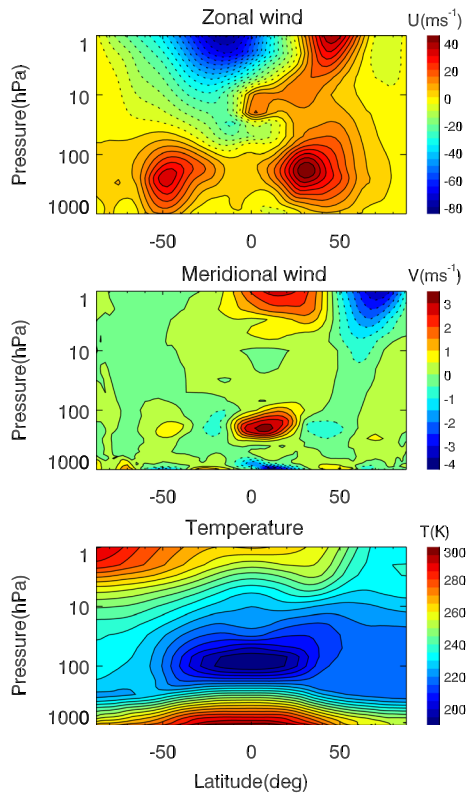

Fig. 1 Monthly averaged zonal-mean zonal wind (top), meridional wind (middle) and temperature (bottom) in January 2013 from the ERA-Interim data

is basically consistent with the monthly climatology for zonal mean temperature structure during SSW events (Seppälä et al. 2013). Therefore, we speculate that SSW may occur in January 2013. Further analyses on the 2012/2013 SSW event would be presented in "The W1 Q16DW during the major SSW in 2012/2013".

To obtain the amplitudes of the Q16DW, we use least square fitting to fit cosine functions to the zonal wind, meridional wind and temperature perturbations in a 32-day window in the data set. At each pressure level, the zonal wind, meridional wind, and temperature data were sorted into latitude bands of 2.5 degrees from 85 °S to 85 °N. The harmonic fitting formula is written as follows:

$$f^{'}(t,\lambda) = \mathrm{A}\cos\left(\frac{2\pi}{\mathrm{T}}\mathrm{t} + \mathrm{s}\lambda - \phi\right) \quad (1)$$

where A, ϕ, T, and s are the amplitude, phase, period and zonal wavenumber of the Q16DW oscillation, respectively. t and λ are the universal time in day and longitude in radians, respectively. To reveal the global characteristics of the Q16DW, we chose zonal wavenumbers from − 6 to 6 to perform the fitting. Here, the positive zonal wavenumbers correspond to westward propagation, and negative zonal wavenumbers correspond to eastward propagation. In each window, the fitting for each zonal wavenumber is performed with the period incrementing by a step of 0.25 days from 12.0 to 20.0 days. At any given pressure level and latitude, the Q16DW amplitude and phase correspond to the one fit among all periods that has the largest amplitude.

To cover the period when the 2012/2013 SSW occurred, we chose the data from December 2012 to November 2013 to study the Q16DW activity in a whole year. Our fitting results show that the Q16DW is generally concentrated in middle and high latitudes in both hemispheres irrespective of the zonal wavenumbers (figures not shown here). In the NH, the westward- and eastward-propagating waves with $s = 1$ and $s = -1$ are evidently larger than other modes, while in the SH, the eastward-propagating waves with $s = -1$ and $s = -2$ have comparable magnitudes and are clearly stronger than the westward-propagating and other eastward-propagating modes. For the zonal/meridional wind, the maximum amplitudes of the $s = 1, -1$ and -2 modes are 30.5/31.4 ms^{-1}, 20.9/22.1 ms^{-1} and 17.2/25.5 ms^{-1}, respectively. The wind amplitudes of other modes are quite small, i.e., only several ms^{-1}. For the temperature, the maximum amplitudes of the $s = 1, -1$ and -2 modes are 17.2 K, 7.5 K and 7.9 K, respectively, and those of the other modes are smaller than 5.0 K. In conclusion, the important modes of the Q16DW in the troposphere and stratosphere are those with $s = 1, -1$ and -2. Compared with the two eastward-propagating modes, the $s = 1$ mode is apparently overwhelming, especially during the period of the 2012/2013 SSW. Therefore, in the following section, we would like to focus on this mode, and reveal its global characteristics.

Seasonal, latitudinal and altitudinal variations of the W1 Q16DW

To investigate the seasonal structure of the W1 mode, we investigated the fitting results of the zonal wind, meridional wind, and temperature during specific months. Figure 2 illustrates the altitude versus latitude structures of the W1 Q16DW amplitudes in January, April, July, and October 2013. The fitting windows are centered on 15.5 January, 15 April, 15.5 July, and 15.5 October. It can be observed that the strongest amplitudes in the zonal wind, meridional wind, and temperature occur in January in the stratosphere of the NH. For the zonal wind, we can see two peaks at 1 hPa with a value of 30.5 ms^{-1} at 85 °N and 20.7 ms^{-1} at 45 °N. For the meridional wind, the maximum amplitude of 31.4 ms^{-1} is located at 1 hPa and 85 °N, while for the temperature, the maximum of 17.1 K occurs at 2 hPa and

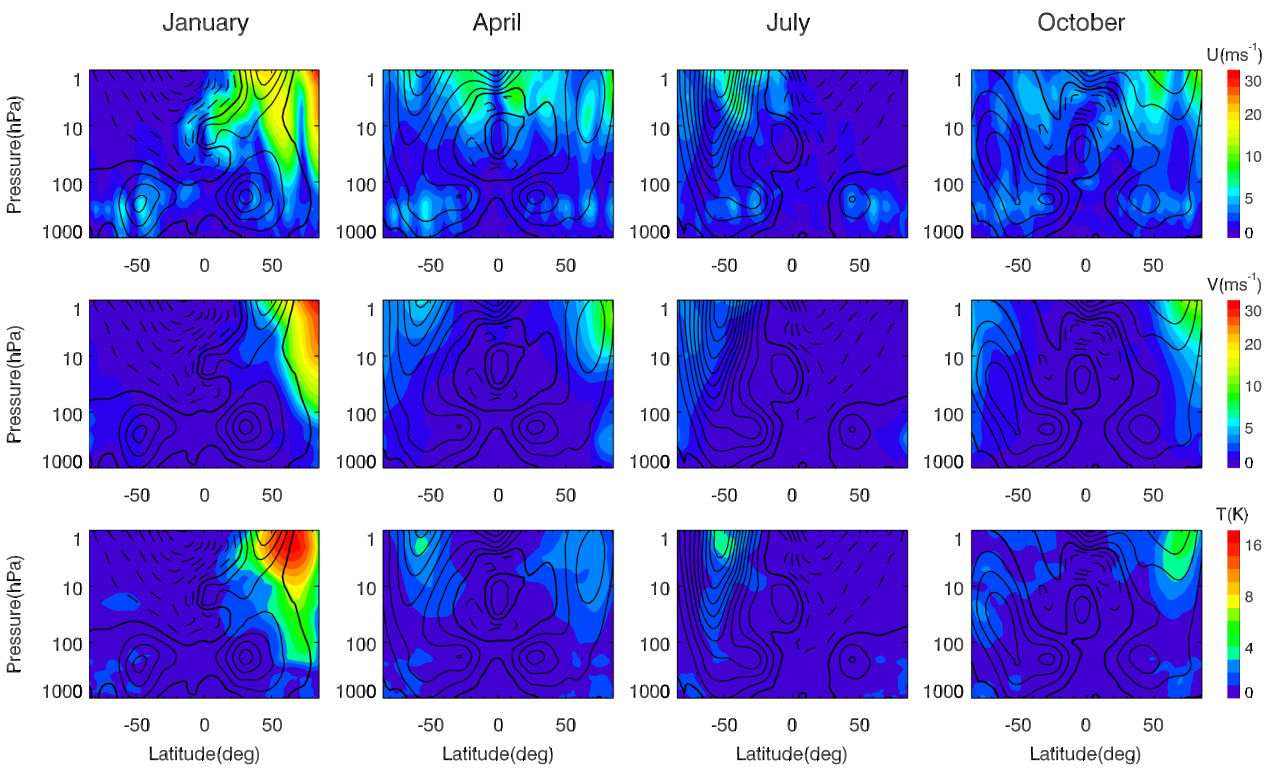

Fig. 2 Altitude versus latitude structures of the W1 Q16DW amplitudes for the zonal wind (top), meridional wind (middle) and temperature (bottom) in January (first column), April (second column), July (third column) and October (last column). In addition, the monthly averaged zonal-mean zonal winds are plotted as contour lines (solid and dashed contour lines represent the eastward and westward winds, respectively, and the thick lines represent zero wind lines) in these months for reference, and the intervals of the contour lines are 10 ms^{-1}

65 °N. Such a strong planetary wave can be related to the interaction with the zonal-mean flow and the polar vortex (Charney and Drazib 1961; Perlwitz and Graf 2001), and it can be a major forcing of the stratospheric dynamics during the winter in the NH. Except for the abnormally strong wave activity in the NH in January, the W1 mode is nonnegligible in the SH in July, and the maximum amplitudes in the zonal wind, meridional wind and temperature are 7.2 ms^{-1}, 4.0 ms^{-1}, and 3.8 K, respectively. At equinoxes (April and October), the W1 mode is active in both hemispheres, while larger amplitudes favor the NH, especially in October, when the maximums for the zonal wind, meridional wind, and temperature are 11.4 ms^{-1}, 12.2 ms^{-1}, and 5.1 K, respectively. Although the largest amplitudes occur in the stratosphere, it is still necessary to investigate the wave activity in the troposphere. In the troposphere, the zonal wind amplitudes are notable for all months in both hemispheres. The meridional wind and temperature components are very weak and have similar magnitudes for all months in both hemispheres. Figure 2 also shows that wave amplitudes in the horizontal wind and temperature are usually very small at equator in all months.

The monthly averaged zonal-mean zonal wind, as the background wind, is also shown in Fig. 2. The background wind contour interval is 10 ms^{-1}, with solid lines denoting the eastward winds, dashed lines denoting the westward winds, and thick lines denoting zero wind lines. In the troposphere, a strong eastward zonal wind exists in both hemispheres in all months, which coincides with the notable zonal wind amplitude of the wave. Since the stratospheric wave activity is particularly intense, we will focus on the relationship between the wind distribution and wave amplitude in the stratosphere. Strong eastward and westward winds exist in the winter and summer hemispheres, respectively. At the equinoxes, the weak eastward wind presents at mid-high latitudes in both the hemisphere and near the equator, and the weak westward wind presents at low latitudes and near the equator. Comparing the W1 Q16DW amplitude with the background wind in the stratosphere, we find that the active waves are mostly coincident with the eastward mean zonal flows. Therefore, the seasonal structures of

the W1 mode are closely related to the distribution of the background zonal wind in the stratosphere. Theoretically, it is already well established that the Q16DW preferentially propagates in an eastward background flow. However, note that the eastward wind regions are not filled with wave activity and that wave activity does occur in the weak westward flows. In January 2013, we suggest that the weak westward flow near the Arctic is associated with the strong W1 mode, which will be discussed in the next section. For the zonal wind component, there are also weak W1 modes present in the weak westward wind at low latitudes, which is consistent with the previous observational study by Luo et al. (2002). These results indicate that the real atmosphere is more complex than the theoretical situation.

Since strong wave activities take place around the height of 1 hPa, we show the latitude versus month-of-year structures of the W1 Q16DW amplitudes in the zonal wind, meridional wind, and temperature at 1 hPa in Fig. 3. As seen from the figure, there is a clear seasonal cycle in the wave amplitude. The W1 mode is much stronger in the winter hemisphere than in the summer hemisphere at solstices. In the winter hemisphere, it is particularly strong in the NH, while significant but not very strong in the SH. In the NH, the maximum amplitudes in all components are concentrated at middle and high latitudes. In the SH, large zonal wind amplitudes occur at low and middle latitudes, large meridional wind amplitudes are concentrated at middle and high latitudes, and large temperature amplitudes are present at middle latitudes. In spring and autumn, the W1 mode in all components is notable in both hemispheres. The distribution of the amplitudes in Figs. 2 and 3 clearly shows that this wave is not entirely symmetric about the equator at equinoxes.

Previous studies of the Q16DW in the stratosphere have reported waves with large amplitudes during wintertime (Madden and Lindzen 1981; Alexander and Shepherd 2010; Day et al. 2011), which is consistent with our results. Since most of the large amplitudes occur in the NH, we provide the altitude versus month-of-year plots of the W1 Q16DW for the zonal wind, meridional wind and temperature amplitudes at 25 °N, 45 °N, 65 °N and 85 °N in Fig. 4. Consistent with the results shown in Figs. 2 and 3, the largest amplitudes of the W1 Q16DW can also be observed in the stratosphere in the winter months. At high latitudes (65 °N and 85 °N), the maximum magnitudes in all components appear at 1 hPa in January. At 85 °N, the maximum wind amplitudes are very notable, while the maximum temperature amplitudes are not as strong. At 65 °N, the temperature maximums are very notable, while the wind maximums are not as strong as those at 85 °N. In middle latitudes (45 °N), the zonal wind and temperature amplitudes are significant, while the meridional wind component is weak. In low latitudes (25 °N), the zonal wind amplitudes are still significant, while the temperature amplitudes are weak and the meridional wind amplitudes are negligible. In the spring and autumn, significant zonal wind, meridional wind, and temperature amplitudes can be observed at all latitudes, at high latitudes, and at middle and high latitudes, respectively. In the troposphere, the largest amplitudes in all components are located at 85 °N. At 25 °N, 45 °N and 65 °N, the zonal wind components are weak, while both the meridional wind and temperature components are negligible. In addition, Figs. 3 and 4 show that the stratospheric amplitudes in the NH are significantly reduced in February following a major SSW, which is consistent with an earlier study by Day et al. (2011).

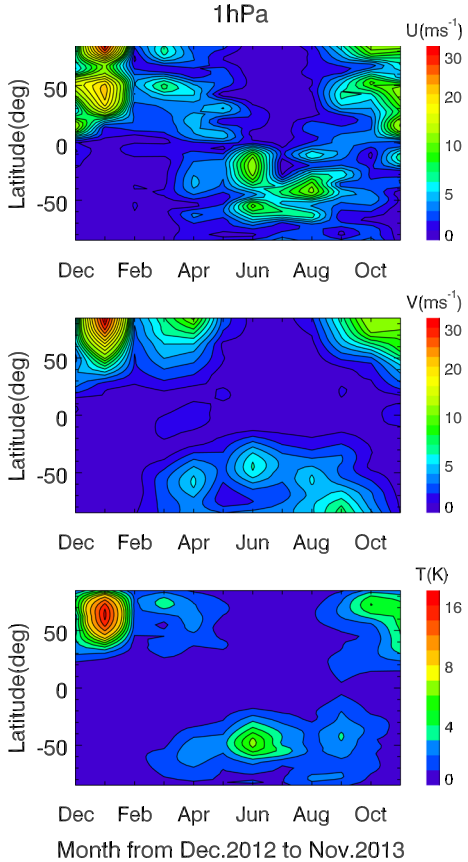

Fig. 3 Latitude versus month-of-year structures of the W1 Q16DW amplitudes for the zonal wind (top), meridional wind (middle) and temperature (bottom) at 1 hPa

In conclusion, the W1 mode is evidently stronger in the stratosphere than in the troposphere. In the stratosphere, it is very strong in winter, significant in spring and autumn, and negligible in summer. The zonal wind

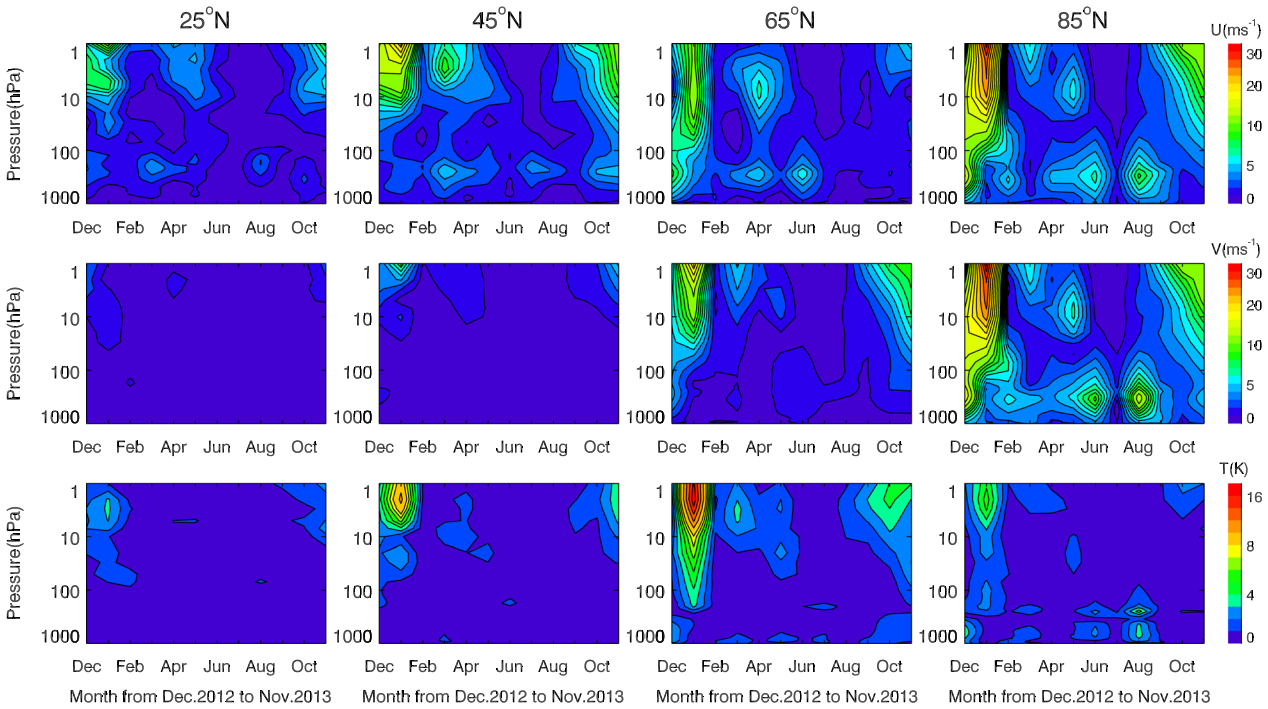

Fig. 4 Altitude versus month-of-year structures of the W1 Q16DW amplitudes for the zonal wind (top), meridional wind (middle) and temperature (bottom) at 25 °N (first column), 45 °N (second column), 65 °N (third column) and 85 °N (last column)

maximum amplitudes are located at 45 °N and in the polar region, the meridional wind amplitudes occur in the polar region, while the temperature amplitudes are concentrated at 65 °N. In the troposphere, the W1 mode did not display evident seasonal variation.

The W1 Q16DW during the major SSW in 2012/2013

It is found that in the whole year from December 2012 to November 2013, the W1 Q16DW is extraordinarily intense at middle and high latitudes in the stratosphere of the NH in January, when a major SSW event is taking place. Next, we would like to investigate the relationship between the wave amplification and this major SSW event.

The World Meteorological Organization (WMO) defines a major SSW event as the gradient of the temperature from 60 N° to the pole being positive and the reversal of the zonal-mean zonal wind at 10 hPa or below during wintertime. The day when the zonal-mean zonal wind reverses at 10 hPa is taken as the central date of the major SSW event. The major SSW event during the winter of 2012/2013 has been studied for several years (Wit et al. 2014, 2015; Coy and Pawson 2015). Here, we exhibit this event in detail by using the ERA-Interim data. Figure 5 displays the altitude-time cross-section of the

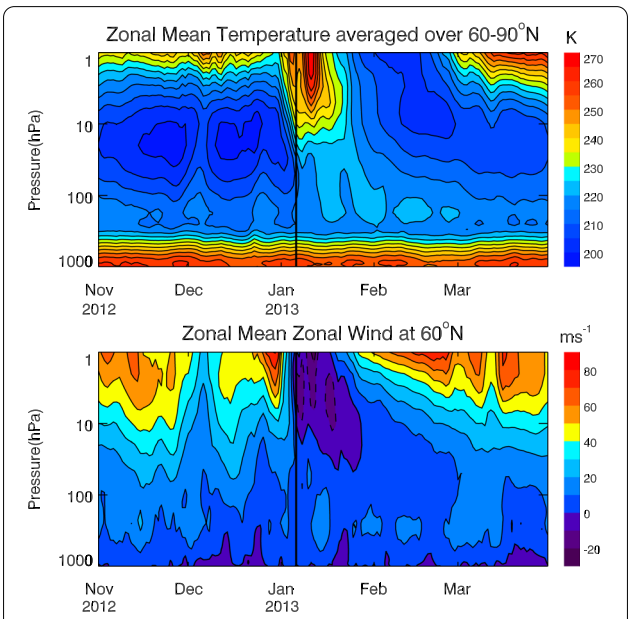

Fig. 5 Altitude-time cross-sections of the zonal-mean temperature averaged from 60 °N to 90 °N (top) and zonal-mean zonal wind at 60 °N (bottom) during the winter of 2012/2013. The thick vertical line denotes 6 January 2013, which is the SSW central date

zonal-mean temperature averaged from 60 °N to 90 °N and the zonal-mean zonal wind at 60 °N from November 2012 to March 2013. The stratospheric temperature rises rapidly after 1 January and reaches a maximum of 267 K at 1 hPa on 11 January. The rapid deceleration of the zonal-mean zonal wind at 60 °N starts when the stratospheric temperature increases rapidly, and then, the wind reverses and remains westward until approximately 27 January. The zonal-mean zonal wind reverses from eastward to westward at 10 hPa and 60 °N on 6 January, so we choose this day as the central date.

To classify the 2012/2013 SSW event, we present the evolutions of stratospheric PV (in units of PVU) and geopotential height around the central date from the ERA-Interim data. An overview of the vortex evolution in the middle (850 K, ~ 10 hPa) and lower (530 K, ~ 50 hPa) stratospheres during the 2012/2013 SSW event is shown in Fig. 6. The PV fields at 850 K (~ 10 hPa) together with the 10 hPa geopotential height show a clear synoptic evolution of the polar vortex in the top panel of Fig. 6. The strong polar vortex with high PV values accompanied by low geopotential heights (black contour) began to shrink and shift off the pole from 28 December 2012 to 2 January 2013, while the weak polar vortex with low PV values accompanied by high geopotential heights (white contour) shifted from low latitudes to middle latitudes. Then, the low PV region (accompanied by high geopotential heights) moved from middle latitudes to the pole, and the high PV region (accompanied by low geopotential heights) began to split on 7 January 2013. The vortex was completely split into two fragments on 12 January 2013. At the bottom panel, similar phenomena can be seen: the strong polar vortex with high PV values accompanied by low geopotential heights (black contour) shifted to the adjacent mid-high latitudes, and then, the vortex split into two fragments. In summary, the lower and middle stratospheric polar vortices first shifted off the pole and then split into two pieces, classifying this major SSW event as a complex event.

According to the results in "Seasonal, latitudinal and altitudinal variations of the W1 Q16DW", we found that the W1 mode of the Q16DW was very energetic in January 2013. To further confirm the dominant traveling PWs in this SSW event, we applied the two-dimensional Fourier transform methods to the ERA-Interim data in January 2013. Figure 7 shows the frequency-wavenumber spectral results of the geopotential height, zonal wind and meridional wind at 1 hPa and 80 °N in January 2013. For each physical quantity, there are two conspicuous peaks at zero frequency with the same amplitudes, which represent the quasi-stationary PWs (Pogoreltsev et al. 2009). SPW1 is the strongest, which will be taken into consideration in the following analyses. In addition, there are significant spectral peaks in all three physical quantities, corresponding to the W1 mode of the Q16DW. For the geopotential height, zonal wind and meridional wind, the strongest spectral peaks have amplitudes of 308 m, 18.5 ms^{-1} and 19.4 ms^{-1}, respectively. For the zonal wind and meridional wind, there are also spectral peaks corresponding to the $s = -1$ mode of the Q16DW, which is

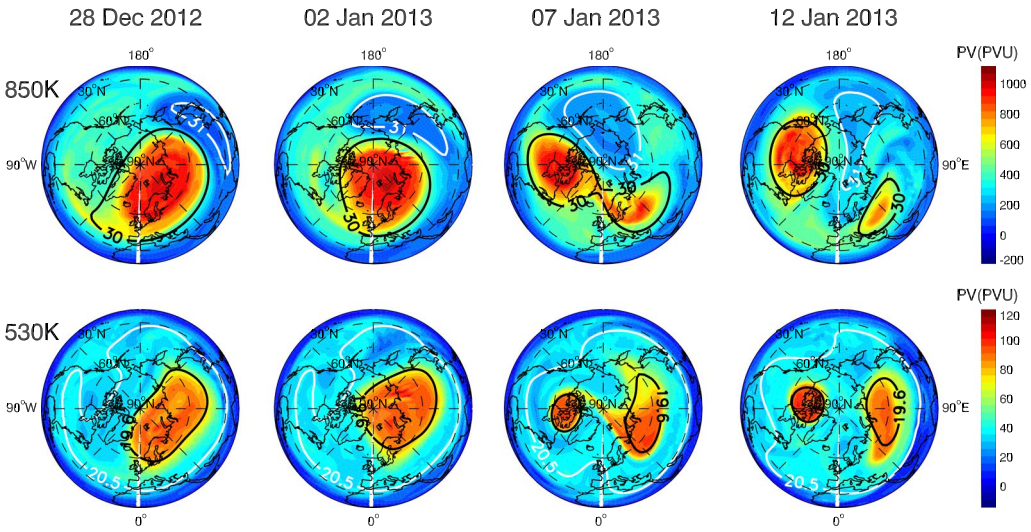

Fig. 6 Maps of potential vorticity (in PVU where 1 PVU $=10^{-6} K kg^{-1} m^2 s^{-1}$) at 850 K (top) and 530 K (bottom) potential temperature surface on 28 December 2012, 2 January 2013, 7 January 2013 and 12 January 2013 (from left to right) in the NH. The overlaid contour represents the geopotential heights at 10 hPa (top) and 50 hPa (bottom), where the black and white solid thick lines denote different values (km). The domain is from the equator to the pole with dashed circles at 30 °N and 60 °N; 0 ° longitude is at the bottom and 90 °E is to the right

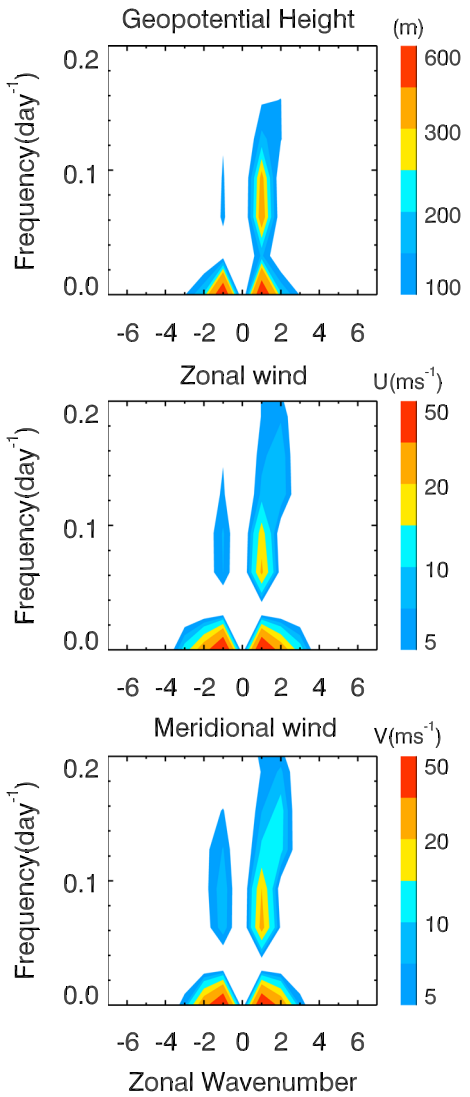

Fig. 7 Frequency–wavenumber spectra of geopotential height (top), zonal wind (middle) and meridional wind (bottom) at 1 hPa and 80 °N in January 2013

much weaker than those for the W1 mode. Therefore, we still focus on the W1 mode in the following paper.

The above spectral analysis indicates that the W1 mode of the Q16DW is likely to be closely related to the 2012/2013 SSW event. To further clarify this relevance, we will display the W1 Q16DW activity during the 2012/2013 SSW event in detail in the following section. We fit the geopotential height, zonal wind and meridional wind data with the zonal wavenumber s = 1 from the equator to 80 °N in a 32-day window, and this window is moved from December 2012 to February 2013 with steps of 1 day to obtain daily values of the wave amplitudes and phases. Figure 8 presents the latitude-time structures of the W1 Q16DW amplitudes in the geopotential height, zonal wind and meridional wind at three pressure levels: 1 hPa, 10 hPa, and 30 hPa. For the geopotential height, the maximum amplitudes are centered near 70 °N at all levels, and the greatest value (930 m) is located at 1 hPa. For the zonal wind, the maximum amplitudes are centered near 40–50 °N and near the Northern Pole, while for the meridional wind, the maximums are near the Northern Pole. The maximum zonal/meridional wind is 31.9/34.7 ms^{-1} and located near the Northern Pole. All the amplitudes in the geopotential height, zonal wind and meridional wind reach their maximums at high latitudes near the central date of the 2012/2013 SSW event, indicating that there is some close connection between the W1 Q16DW activity and the 2012/2013 SSW. Coy and Pawson (2015) found that the upward wave activity flux from the upper troposphere displaces the polar vortex in an SPW1 pattern. The vertical EP flux maximum from SPW2 at 100 hPa averaged over 30–90 °N is less than $1 \times 10^5 kgs^{-2}$, which is smaller than what is found during the previous split SSW events examined by Harada et al. (2010). Therefore, there may exist a wave that is expected to provide an additional forcing to split the polar vortex. The W1 mode is clearly amplified before and during the splitting of the displaced vortex, similar to the amplification of SPW2 described by Coy and Pawson (2015). This indicates that the W1 mode most likely contributes to the breakdown of the polar vortex.

On the central date, the maximum amplitude of geopotential height is found at 65 °N. To determine the vertical propagation characteristics of the W1 mode, we show the profiles of the fitted amplitudes and phases of geopotential height at 65 °N in Fig. 9. The amplitude increases with height. It is worth noting that the phase exhibits a tendency of downward phase progression, indicating that the W1 mode wave propagates upward from lower stratosphere. In addition, the expected amplitude of the theoretical Lamb mode (dashed black line) is also plotted in Fig. 9 (left). We assume that the excepted amplitude has the same value as the actual amplitude at 30 hPa. The expected geopotential height amplitude change is proportional to $e^{(\kappa z/H)}$ based on the log-pressure vertical coordinate z, where κ is the ratio of R the gas constant to c_p the specific heat at constant pressure for air, and H is the scale height. The amplitude of the theoretical Lamb mode throughout the stratosphere shows a linear increasing trend. However, the actual geopotential height amplitude is much larger than the theoretical one, indicating that the W1 Q16DW is not a pure free mode wave, and there exists a wave source in the stratosphere.

The key mechanism for generating a major SSW event is the upward-propagating PWs from the troposphere into the stratosphere, which reverse the

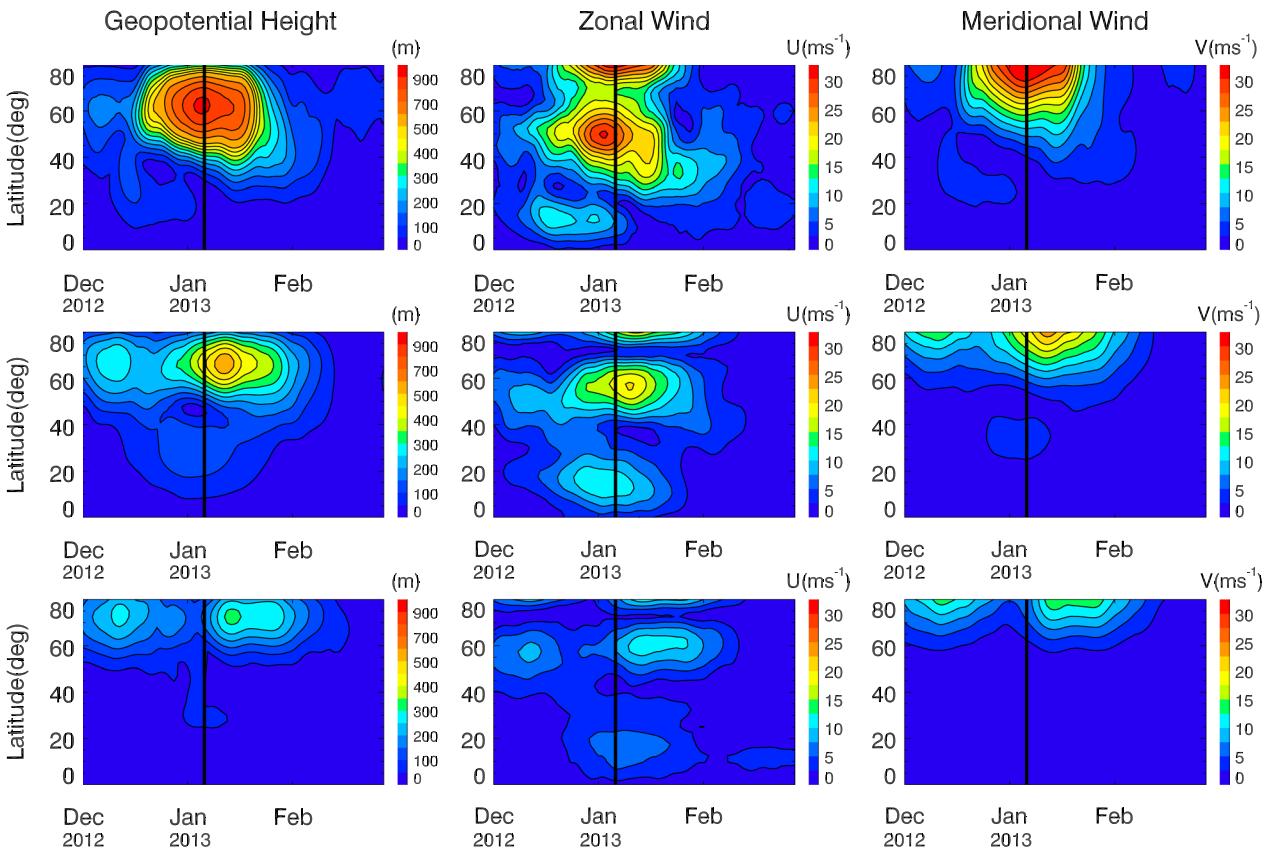

Fig. 8 Latitude versus time structures of the W1 Q16DW amplitudes for the geopotential height (left), zonal wind (middle) and meridional wind (right) at three pressure levels: 1 hPa (top), 10 hPa (middle) and 30 hPa (bottom). The thick vertical line denotes the SSW central date

eastward winter stratospheric jet. The PW activity can also transport a large heat flux to the polar region, which leads to a warmer polar vortex. In our study, it was revealed that the strong W1 Q16DW occurred during the 2012/2013 SSW event. Therefore, we would focus on the interaction of the W1 mode wave with the mean flow in the stratosphere.

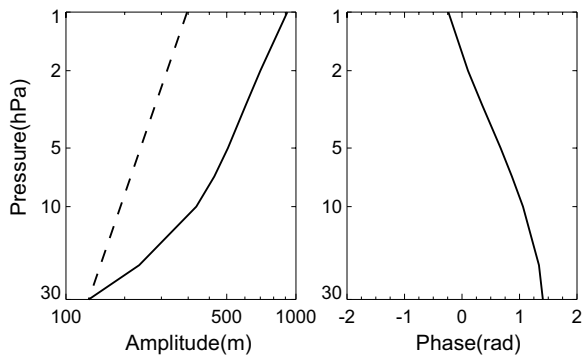

Fig. 9 The amplitudes (left) and phases (right) for the geopotential height at 65 °N. The dashed black line (left) denotes the theoretical expectation of the Lamb mode

The EP flux and its divergence are used to investigate the propagation of eddy momentum and heat of waves and the wave forcing on the mean flow (Chen and Huang 2002; Chen et al. 2002; Tomikawa et al. 2012; Harda and Hirooka 2017; Rodas and Pulido 2017). In this paper, the transformed Eulerian-mean equations in spherical coordinates (Andrews et al. 1987) are applied:

$$\overline{u}_t = -\overline{v}^* \left[\frac{1}{a\cos\varphi} (\overline{u}\cos\varphi)_\varphi - f_0 \right] - \overline{w}^* \overline{u}_z + \frac{1}{\rho_0 a\cos\varphi} \nabla \cdot \mathbf{F} \tag{2}$$

where ρ_0 is the air density, a is the radius of the Earth, φ is the latitude, $f_0 = 2\Omega\sin\varphi$ ($\Omega = 7.292 \times 10^{-5} rads^{-1}$ is the Earth's rotation rate) is the Coriolis parameter, and $u/v/w$ is the zonal/meridional/vertical wind. Here, the zonal-mean fields and partial derivatives are denoted by overbars and subscripts, respectively. The left-hand side of Eq. (2) is the tendency of the zonal-mean zonal wind. The first and second terms on right-hand side represent

accelerations associated with the residual velocities $\overline{v}^*$ and $\overline{w}^*$, which are defined as

$$\overline{v}^* = \overline{v} - \frac{1}{\rho_0}\left(\rho_0 \frac{\overline{v'\theta'}}{\overline{\theta}_z}\right)_z \tag{3}$$

$$\overline{w}^* = \overline{w} + \frac{1}{a\cos\varphi}\left(\cos\varphi \frac{\overline{v'\theta'}}{\overline{\theta}_z}\right)_\varphi \tag{4}$$

where θ is the potential temperature. Here, perturbation quantities are denoted by primes. $\mathbf{F} = \left(0, F^{(\varphi)}, F^{(z)}\right)$ is the EP flux which is a vector in the meridional plane.

The meridional and vertical components of the EP flux in the spherical geometry can be expressed as follows:

$$F^{(\varphi)} = \rho_0 a\cos\varphi\left(\frac{\overline{v'\theta'}}{\overline{\theta}_z}\overline{u}_z - \overline{u'v'}\right) \tag{5}$$

$$F^{(z)} = \rho_0 a\cos\varphi\left\{\left[f_0 - \frac{(\overline{u}\cos\varphi)_\varphi}{a\cos\varphi}\right]\frac{\overline{v'\theta'}}{\overline{\theta}_z} - \overline{u'w'}\right\} \tag{6}$$

The EP flux divergence is given by the following equation:

$$\nabla\cdot\mathbf{F} = \frac{1}{a\cos\varphi}\frac{\partial}{\partial\varphi}\left(F^{(\varphi)}\cos\varphi\right) + \frac{\partial}{\partial z}F^{(z)} \tag{7}$$

The third term on the right side of Eq. (2) is defined as the zonal force per unit mass acting on the mean state $D_F = (\rho_0 a\cos\varphi)^{-1}\nabla\cdot\mathbf{F}$.

For the EP flux, the meridional component indicates the eddy momentum flux, and the vertical component represents the eddy heat flux. D_F can represent the acceleration or deceleration of the zonal-mean flow. The EP flux divergence (positive value) is related to the eastward acceleration by wave activities, while convergence (negative value) is related to the westward acceleration.

Previous study has investigated the contributions of different waves to the EP flux and found that the EP flux is mostly due to the PWs in the stratosphere (Tomikawa et al. 2012). Hirooka (1986) found that the interference between traveling and quasi-stationary PWs can produce periodic changes of EP flux and its divergence, which in turn give rise to the vacillations in the basic flow. Since the amplitude of the traveling PWs is of the same order of magnitude as that of quasi-stationary PWs, Hirooka and Hirota (1985) indicated that the interference between traveling and quasi-stationary wave may plays an important role in the SSW event. The meridional wind amplitudes of W1 mode have comparable magnitudes with the quasi-stationary PWs described by Coy and Pawson (2015). Coy and Pawson (2015) revealed that SPW1 and SPW2 played a key role during this SSW event. Therefore, we speculate that the W1 mode may interact with the SPW1 during the 2012/2013 SSW event. This interaction would be discussed in detail in the following part. Hereafter, we use W1-SPW1 as the abbreviation for the "interaction between W1 Q16DW and SPW1".

Referring to the previous work (Salby and Garcia 1987), we consider the simple two component frequency–wavenumber spectrum (referring to Fig. 7) and let $x' = x'_{Q16DW} + x'_{SPW1}$. Here, $x' = [u', v', w', \theta']$. Then, the total EP flux field can be divided into two groups. The first group is the contribution from each spectral component, i.e., from the Q16DW and the SPW1, respectively. The second is contribution from the interaction of the two spectral components (representing by their cross terms), i.e., from W1-SPW1.

To clarify processes responsible for the zonal wind tendency during the SSW event, each term of Eq. (2) is evaluated. Figure 10 shows the time–pressure sections of the zonal wind tendency ($\overline{u}_t$), the zonal wind acceleration due to D_F, and zonal momentum advection due to residual meridional and vertical velocities at 50–80 °N. Here, the zonal wind acceleration due to D_F is calculated from the total EP flux. The $\overline{u}_t$ is determined by the residual between the D_F and momentum transport due to the meridional circulation. As shown in Fig. 10, D_F and the meridional advection are dominant and tend to cancel each other during the 2012/2013 SSW event. Contributions of the vertical advection are quite small. As a result, the $\overline{u}_t$ is roughly given as a small residual between D_F and the meridional advection. Before the central date, large negative EP flux divergences are observed in the middle and high stratosphere. Just after the central date, it is interesting that large negative and positive EP flux divergences appear above and below 2 hPa, respectively. Then, large EP flux convergences appear above 2 hPa. These large EP flux convergences are largely canceled by meridional advection. During the 2012/2013 SSW, the zonal wind tendency follows the sign of the D_F in most of the height range. Therefore, the zonal wind tendency is roughly dominated by the EP flux divergence.

Figure 11 shows the time–pressure sections of D_F due to quasi-stationary planetary waves/the interaction between quasi-stationary planetary waves and W1 Q16DW/W1 Q16DW at 50–80 °N. In December, the convergence/divergence regions are dominated by quasi-stationary PWs below 2 hPa. Relatively small EP flux convergences from the interaction of quasi-stationary PWs with W1 Q16DW also occur in upper

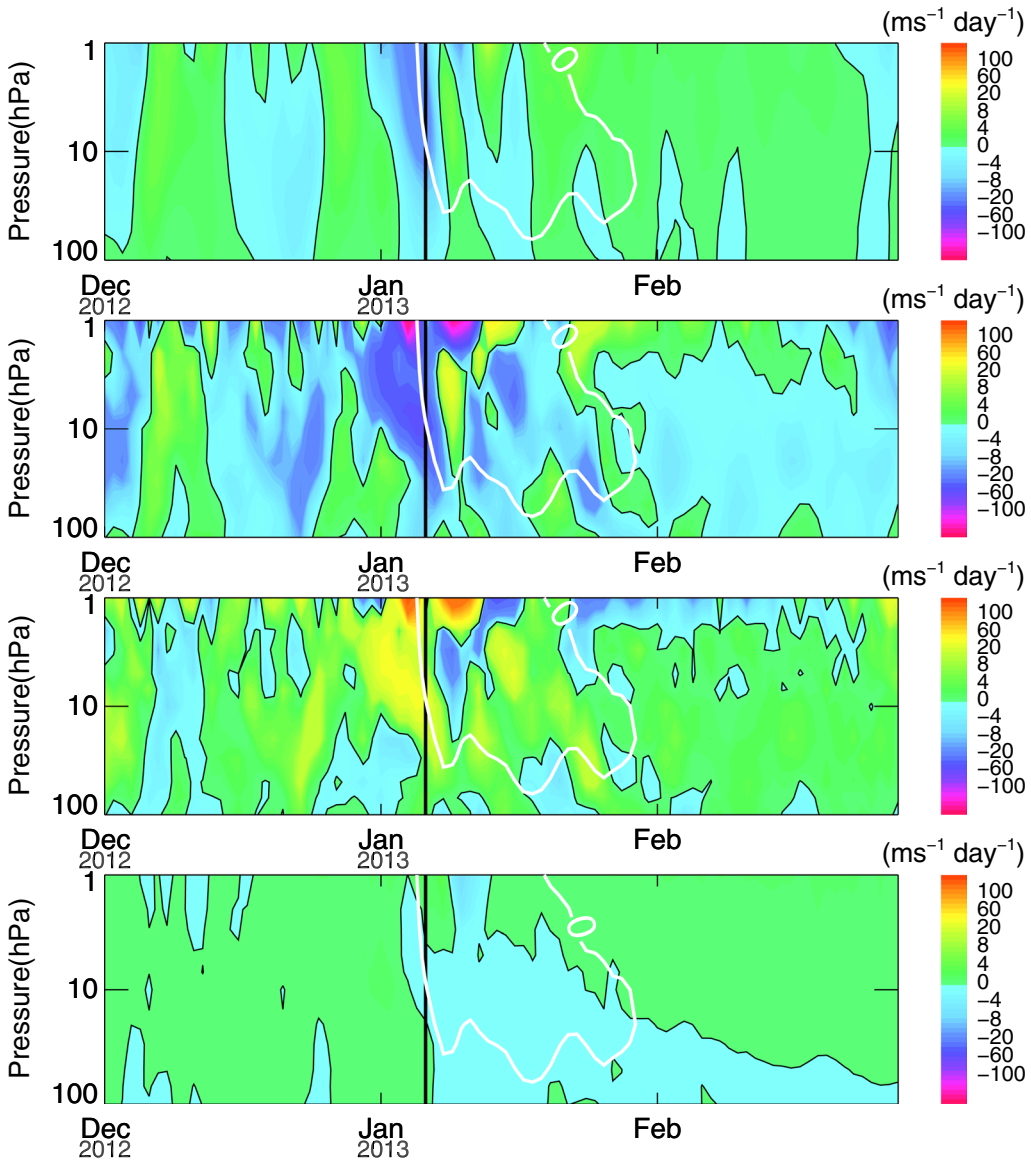

Fig. 10 Latitude versus time structures of the $\overline{u}_t$ (first row), the D_F (second row), the meridional (third row) and vertical (last row) advection of zonal momentum at 50–80 °N. Black thick vertical line denotes the SSW central date. White contours represent zero zonal winds. Black thin contours represent 0 $ms^{-1}day^{-1}$

and middle stratosphere. Around the central date, it is worth noting that both quasi-stationary PWs and interaction component produce large EP flux convergence in the upper stratosphere. Moreover, both negative and positive D_F from W1 Q16DW are particularly small and can be ignored. As a result, a large EP flux convergence associated with the interaction provides an additional contribution to the reversal of eastward wind. Therefore, the interaction between W1 Q16DW and quasi-stationary PWs plays an important role in this SSW event.

Here, we explore the effects of the interaction between the W1 Q16DW and quasi-stationary PWs on the mean flow during the 2012/2013 SSW by calculating the EP flux and its divergence. Figure 12 shows the zonal-mean zonal wind, EP flux vector and D_F from W1-SPW1 on 26 December 2012, 31 December 2012, 5 January 2013, and 10 January 2013. All the strong EP flux vectors are concentrated in mid-high latitudes in the stratosphere. The EP flux vectors show upward propagation in the NH, which is consistent with the W1 mode propagation in Fig. 9. It can be clearly seen that

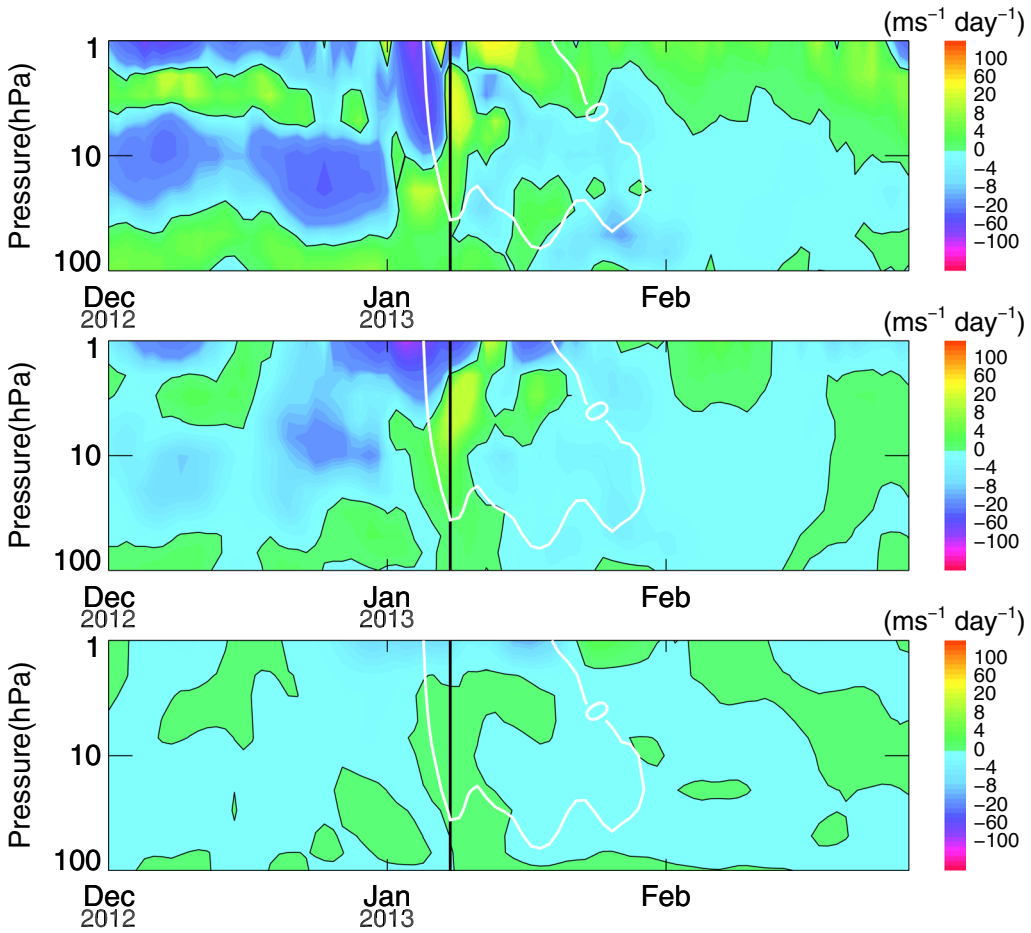

Fig. 11 As in Fig. 10, but for the D_F from quasi-stationary PWs (top), interaction between W1 Q16DW and quasi-stationary PWs (middle), and W1 Q16DW (bottom) at 50–80 °N

the strong W1-SPW1 occurs in the lower stratosphere (below 10 hPa) and gradually extends upward on 5 January 2013. The EP flux vortex from W1-SPW1 become smaller after the central date. Note that the vertical EP flux from W1-SPW1 have the same order of magnitude as that from SPW2 described by Coy and Pawson (2015) at 100 hPa, which provides supplementary evidence for the contribution of the W1 to the splitting of the polar vortex. Importantly, a large heat flux (vertical component of EP flux) due to W1-SPW1 in Fig. 12 can be seen during the 2012/2013 SSW, which is consistent with the increased temperature. This finding indicates that W1-SPW1 may produce adiabatic warming in the stratosphere. Strong EP flux convergence of W1-SPW1 first occurs around high latitude (70–80 °N) on 26 December 2012, and then extends to low latitude (40 °N) on 5 January 2013. These observed strong eddy forcing regions lead to the deceleration and even reversal of the eastward winter stratospheric jet. It is worth noting that EP flux divergence region exists in the middle stratosphere below the upper stratosphere convergence region.

Figure 13 exhibits the W1 Q16DW amplitudes in the geopotential height, zonal wind and meridional wind. The selected four days in this figure are the same as those in Fig. 12. In the middle and upper stratosphere, the W1 Q16DW amplitudes in the geopotential height, zonal wind, and meridional wind is amplified at mid-high latitudes, which correspond to the strong EP flux in the Fig. 12.

According to the results and discussion above, the dynamic situation can be understood as follows: W1-SPW1 in the stratosphere may contribute greatly to the eastward jet reversal during this SSW event. In addition, this interaction also plays an important role in the stratospheric polar warming. Apparently, part of the W1 Q16DW in the stratosphere is the result of the upward-propagating wave from the low atmosphere. Since the W1 Q16DW is amplified in the stratosphere, there is also a wave source there, which is verified by the EP

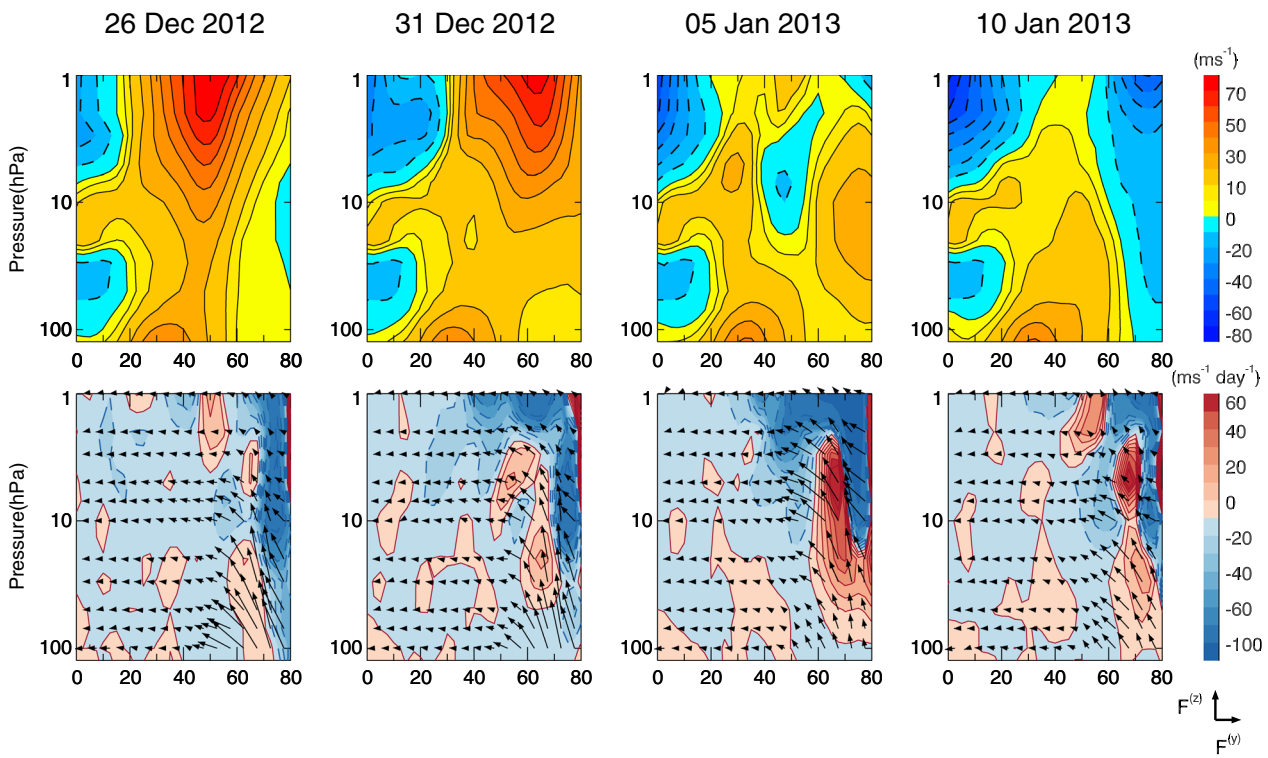

Fig. 12 Altitude versus latitude structures of zonal-mean zonal winds (top), EP flux **F**(vectors) and D_F (color shading) from W1-SPW1 (bottom) in the NH on 26 December 2012, 31 December 2012, 5 January 2013, and 10 January 2013. In the bottom panel, the arrow scales denote 4×10^7 and $2.5 \times 10^5 kgs^{-2}$ for the meridional and vertical components of the EP flux, respectively

flux divergence region in the stratosphere. Thus, the W1 Q16DW in the stratosphere is the sum of the upward-propagating wave and the in situ excited wave, which is consistent with the results of Fig. 9.

Next, we explore the forcing mechanisms of the amplified W1 Q16DW in the stratosphere. The observed EP flux divergence region in the stratosphere is a key point of the wave forcing, indicating that there is indeed an in situ wave source. Thus, the possibility of in situ instability is considered and subsequently discussed. The effects of the mean flow on the propagation of the Q16DW can be quantified by the baroclinic and/or barotropic instability. Changes in the sign in the basic northward quasi-geostrophic potential vorticity gradient ($\overline{q}_\varphi$) indicate the necessary conditions for the baroclinic and/or barotropic instability of the mean flow. To investigate this mechanism, we calculated $\overline{q}_\varphi$, which can be expressed in spherical coordinates as follows (Andrews et al. 1987):

$$\overline{q}_\varphi = 2\Omega\cos\varphi - \left[\frac{(\bar{u}\cos\varphi)_\varphi}{a\cos\varphi}\right]_\varphi - \frac{a}{\rho_0}\left(\frac{\rho_0 {f_0}^2}{N^2}\bar{u}_z\right)_z \quad (8)$$

Here, N is the buoyancy frequency. The second and third terms of the right-hand side of Eq. (8) indicate the barotropic and baroclinic instability, respectively. The case when the second term of Eq. (8) dominates the third term is referred to as barotropic instability, and the opposite case is referred to as baroclinic instability.

To further determine the possible relationship between the amplified W1 Q16DW and the instability of the mean flow, Fig. 14 shows the altitude–latitude structures of $\overline{q}_\varphi$ on the same selected days as in Fig. 13. The blue and uncolored regions in Fig. 14 represent the possible mean flow instability regions. Note that the barotropic instability and/or baroclinic instability have roughly equal contributions to the mean flow instability in this case (not shown here). In the upper stratosphere, the W1 Q16DW in the geopotential height, zonal wind, and meridional wind is amplified in mid-high latitudes, which corresponds to the sign-changing region of $\overline{q}_\varphi$. The negative region of $\overline{q}_\varphi$ extends from the upper stratosphere to the lower stratosphere after the central date. In addition, there are significant amplitude regions for the geopotential height, zonal wind and meridional wind in Fig. 13. The distribution of the W1 Q16DW amplitude in the zonal wind is more consistent with the

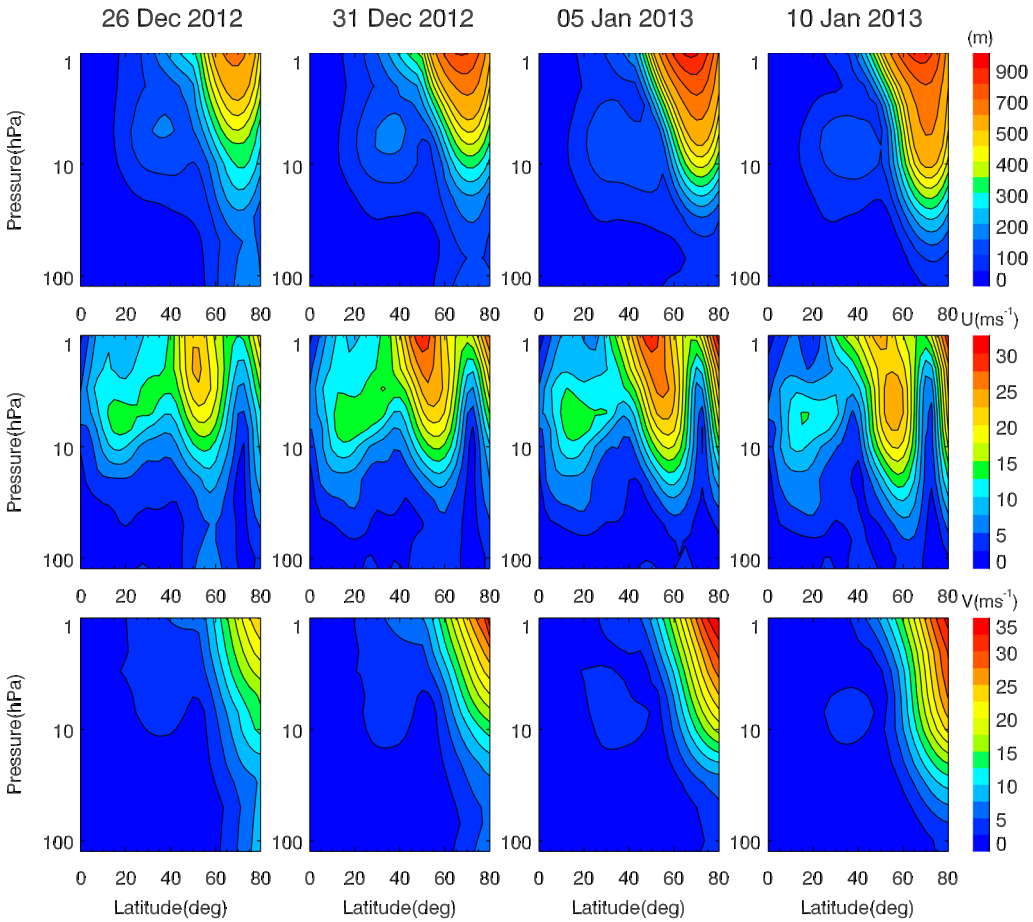

Fig. 13 Altitude versus latitude structures of the geopotential, zonal wind and meridional wind amplitudes of the W1 Q16DW (from top to bottom) in the NH on the same days as those shown in Fig. 12

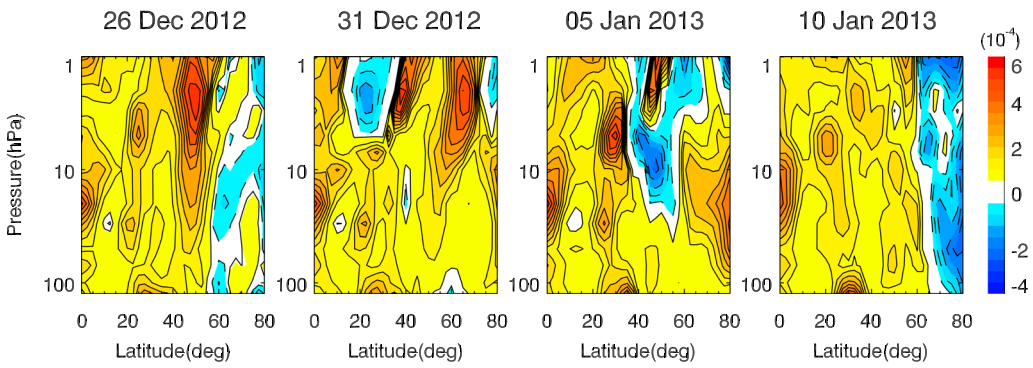

Fig. 14 As in Fig. 13, but for the $\overline{q}_{\varphi}$

instability region than the meridional wind and geopotential height. This difference may be because the curvature terms of the zonal wind are closely related to the second and third terms on the right-hand side of Eq. (6).

In addition, a comparison of Figs. 12 and 14 clearly demonstrates that the negative regions of $\overline{q}_{\varphi}$ correspond to the regions where the eastward winter stratospheric jet reverses and remains westward. The large divergence region occurs where $\overline{q}_{\varphi} < 0$. This result suggests

that in situ instability causes the growth of W1 Q16DW accompanying the large positive EP flux divergence.

In summary, the observed barotropic and/or baroclinic instability of the mean flow in the stratosphere contributes significantly to the enhanced W1 Q16DW or may be an incentive source of the W1 Q16DW.

Summary

Using the ERA-Interim data for one whole year from December 2012 to November 2013, this paper provides insights into the global distribution and seasonal variation in the W1 Q16DW and its dynamic features during the SSW in this year. To our knowledge, this is perhaps the first study to investigate in detail the contribution of the W1 Q16DW to the occurrence of the 2012/2013 SSW event and breakdown of the polar vortex. The main results of this study are summarized as follows.

By checking all the fitting amplitudes of the Q16DW with wavenumbers from -6 to 6, we find that the modes of $s = -2, -1, 1$ are clearly stronger than others. In the NH winter, the quasi-16-day waves with $s = 1$ and $s = -1$ are significant. The eastward-propagating waves with $s = -1$ and $s = -2$ dominate the SH winter. The Q16DW with $s = 1$ was the most prominent, and it is active in middle and high latitudes in the troposphere and stratosphere. In the troposphere, the amplitudes of the $s = 1$ mode in the zonal wind are more significant than those in the meridional wind, and the large amplitudes are located at the altitude where the tropospheric jet is located. In the stratosphere, the W1 Q16DW in the NH is the strongest in winter, significant in spring and autumn, and negligible in summer. However, the amplitude in the SH is negligible in summer and weak in other seasons. In particular, the large amplitudes of the W1 Q16DW in winter are consistent with the presence of primarily eastward prevailing winds that enhance vertical penetration of this westward-propagating wave.

The winter of 2012/2013 is characterized by a major SSW centered on 6 January 2013. The evolutions of the PV and geopotential height field in the lower and middle stratosphere during the 2012/2013 SSW event show that the polar vortex changed from a displacement event to a split event, which is distinct from the typical vortex-displacement-type SSW event and vortex-splitting-type SSW event (Chandran and Collins 2014). During the SSW, the spectral results show that there is a noticeable W1 Q16DW in the stratosphere. We exhibit the latitude-time structures of the W1 Q16DW amplitude in the geopotential height, zonal wind and meridional wind from December 2012 to February 2013 and find that the wave is amplified before and during the 2012/2013 SSW event, similar to SPW2. Together with SPW2, the W1 Q16DW may contribute to this specific and complex split event of the 2012/2013 SSW event.

The interaction between amplified W1 Q16DW and quasi-stationary PWs during the 2012/2013 SSW event may exert a strong forcing on the winter stratospheric mean flow. To confirm this conjecture, we calculate the EP flux and its divergence of W1-SPW1 to investigate the waves forcing on the mean flow. The strong EP flux is centered near mid-high latitudes in the stratosphere. For the vertical component, the W1-SPW1 exhibits a clear upward propagation tendency, indicating that W1 Q16DW originates from the lower atmosphere and interacts with SPW1 in the stratosphere. For the meridional component, all of these interactions occur at mid-high latitudes propagate toward the equator. The strong westward forcing of W1-SPW1 occurs in the stratosphere, indicating that these wave interactions can contribute greatly to the deceleration or even reversal of the eastward stratospheric jet. Furthermore, the W1 Q16DW is excited in the region of strong EP flux convergence, and can be seen at mid-high latitudes in the stratosphere. That is, in addition to the wave that originates from the troposphere, there is also an in situ excited wave.

During this SSW event, we further determined the interaction between the W1 Q16DW and mean flow. The basic northward quasi-geostrophic potential vorticity gradient is calculated to represent the instability of the mean flow. The comparison between the amplification of the W1 Q16DW and the sign-changing region of $\overline{q}_{\varphi}$ suggests that the barotropic instability and/or baroclinic instability may be an in situ wave source. The increase and strong EP flux is consistent with the mean flow instability region, which also confirms that the barotropic instability and/or baroclinic instability contributes to the growth of waves. Therefore, in addition to the upward-propagating W1 Q16DW from the lower atmosphere in the above section, the mean flow instability in the stratosphere can provide additional and essential sources for the amplification of the W1 Q16DW.

Abbreviations

Q16DW: Quasi-16-day wave; W1: Zonal wavenumber 1; ECMWF: European Centre for Medium-Range Weather Forecasts; ERA: ECMWF Interim Re-Analysis; NH: Northern Hemisphere; SH: Southern Hemisphere; SSW: Stratospheric Sudden Warming; PWs: Planetary waves; EP: Eliassen–Palm; SPW1: Quasi-stationary planetary waves with a zonal wavenumber of 1; SPW2: Quasi-stationary planetary waves with a zonal wavenumber of 2; PV: Potential vorticity.

Acknowledgements

This work was jointly supported by the National Natural Science Foundation of China (through grants 41874178, 41531070 and 42074182). We thank ECMWF for the dissemination of the ERA-Interim data.

Authors' contributions

WL analyzed the data and drafted the manuscript. WL and CH contributed to the development of the method. WL, CH and SZ performed analyses related

to the present study, and interpreted the results. All the authors read and approved the final manuscript.

Funding
This work was jointly supported by the National Natural Science Foundation of China (41874178, 41531070 and 42074182).

Availability of data and materials
The ERA-Interim data are provided by ECMWF and available at https://www.ecmwf.int/.

Declarations

Competing interests
The authors declare that they have no competing interests.

Author details
[1]School of Electronic Information, Wuhan University, Wuhan, Hubei, China. [2]Key Laboratory of Geospace Environment and Geodesy, Ministry of Education, Wuhan, Hubei, China. [3]State Key Laboratory of Information Engineering in Surveying, Mapping, and Remote Sensing, Wuhan University, Wuhan, Hubei, China.

Received: 29 October 2020 Accepted: 4 May 2021
Published online: 24 May 2021

References

Alexander SP, Shepherd MG (2010) Planetary wave activity in the polar lower stratosphere. Atmos Chem and Phys 10(2):707–718. https://doi.org/10.5194/acp-10-707-2010
Andrews DG, Holton JR, Leovy CB (1987) Middle Atmosphere Dynamics. Academic Press Inc, New York
Bancalá S, Krüger K, Giorgetta M (2012) The preconditioning of major sudden stratospheric warmings. J Geophys Res 117:D04101. https://doi.org/10.1029/2011JD016769
Butler AH, Sjoberg JP, Seidel DJ, Rosenlof KH (2017) A sudden stratospheric warming compendium. Earth Syst Scie Data 9(1):63–76. https://doi.org/10.5194/essd-9-63-2017
Chandran A, Collins RL (2014) Stratospheric sudden warming effects on winds and temperature in the middle atmosphere at middle and low latitudes: a study using WACCM. Ann Geophys 32(7):859–874. https://doi.org/10.5194/angeo-32-859-2014
Charlton AJ, Polvani LM (2007) A New Look at Stratospheric Sudden Warmings. Part I: Climatology and modeling benchmarks. J Climate 20(3):449–469. https://doi.org/10.1175/JCLI3996.1
Charney JG, Drazin PG (1961) Propagation of planetary-scale disturbances from the lower into the upper atmosphere. J Geophys Res 66(1):83–109. https://doi.org/10.1029/JZ066i001p00083
Chen W, Huang R (2002) The propagation and transport effect of planetary waves in the Northern Hemisphere winter. Adv Atmos Sci 19(6):1113–1126. https://doi.org/10.1007/s00376-002-0069-x
Chen W, Graf H-F, Masaaki T (2002) Observed interannual oscillations of planetary wave forcing in the Northern Hemisphere winter. Geophys Res Lett 29(22):2073. https://doi.org/10.1029/2002GL016062
Chen G, Wu C, Zhang S, Ning B, Huang X, Zhong D, Qi H, Wang J, Huang L (2016) Midlatitude ionospheric responses to the 2013 SSW under high solar activity. J Geophys Res Space Phys 121(1):790–803. https://doi.org/10.1002/2015JA021980
Coy L, Pawson S (2015) The major stratospheric sudden warming of January 2013: analyses and forecasts in the GOES-5 data assimilation system. Mon Wea Rev 143:491–510. https://doi.org/10.1175/MWR-D-14-00023.1
Coy L, Eckermann S, Hoppel K (2009) Planetary wave breaking and tropospheric forcing as seen in the stratospheric sudden warming of 2006. J Atmos Sci 66(2):495–507. https://doi.org/10.1175/2008JAS2784.1
Daley R, Williamson DL (1985) The existence of free Rossby waves during January 1979. J Atmos Sci 42(20):2121–2141. https://doi.org/10.1175/1520-0469(1985)042%3c2121:TEOFRW%3e2.0.CO;2
Day KA, Mitchell NJ (2010) The 16-day wave in the Arctic and Antarctic mesosphere and lower thermosphere. Atmo Chem and Phys 10(3):1461–1472. https://doi.org/10.5194/acp-10-1461-2010
Day KA, Hibbins RE, Mitchell NJ (2011) Aura MLS observations of the westward-propagating s=1, 16-day planetary wave in the stratosphere, mesosphere and lower thermosphere. Atmos Chem and Phys 11(9):4149–4161. https://doi.org/10.5194/acp-11-4149-2011
de Wit RJ, Hibbins RE, Espy PJ, Orsolini YJ, Limpasuvan V, Kinnison DE (2014) Observations of gravity wave forcing of the mesopause region during the January 2013 major sudden stratospheric warming. Geophys Res Lett 41(13):4745–4752. https://doi.org/10.1002/2014GL060501
de Wit RJ, Hibbins RE, Espy PJ, Hennum EA (2015) Coupling in the middle atmosphere related to the 2013 major sudden stratospheric warming. Ann Geophys 33(3):309–319. https://doi.org/10.5194/angeo-33-309-2015
Dee DP, Uppala SM, Simmons AJ, Berrisford P, Poli P, Kobayashi S, Andrae U, Balmaseda MA, Balsamo G, Bauer P, Bechtold P, Beljaars ACM, van de Berg L, Bidlot J, Bormann N, Delsol C, Dragani R, Fuentes M, Geer AJ, Haimberger L, Healy SB, Hersbach H, Hólm EV, Isaksen L, K å llberg P, Köhler M, Matricardi M, McNally AP, Monge-Sanz BM, Morcrette J-J, Park B-K, Peubey C, de Rosnay P, Tavolato C, Thépaut J-N, Vitart F, (2011) The ERA-Interim reanalysis: configuration and performance of the data assimilation system. Quart J Roy Meteor Soc 137(656):553–597. https://doi.org/10.1002/qj.828
Dunkerton TJ (1991) LIMS (Limb Infrared Monitor of the Stratosphere) observation of traveling planetary waves and potential vorticity advection in the stratosphere and mesosphere. J Geophys Res Atmos 96(D2):2813–2834. https://doi.org/10.1029/90JD02340
Flannaghan TJ, Fueglistaler S (2011) Kelvin waves and shear-flow turbulent mixing in the TTL in (re-)analysis data. Geophys Res Lett 38(2):L02801. https://doi.org/10.1029/2010GL045524
Forbes JM, Zhang X (2015) Quasi-10-day wave in the atmosphere. J Geophys Res Atmos 120(21):11079–11089. https://doi.org/10.1002/2015JD023327
Forbes JM, Hagan ME, Miyahara S, Vial F, Manson AH, Meek CE, Portnyagin YI (1995) Quasi 16-day oscillation in the mesosphere and lower thermosphere. J Geophys Res Atmos 100(D5):9149–9163. https://doi.org/10.1029/94JD02157
Garcia RR (1987) On the mean meridional circulation of the middle atmosphere. J Atmos Sci 44(24):3599–3609. https://doi.org/10.1175/1520-0469(1987)044%3c3599:OTMMCO%3e2.0.CO;2
Gómez-Escolar M, Calvo N, Barriopedro D, Fueglistaler S (2014) Tropical response to stratospheric sudden warmings and its modulation by the QBO. J Geophys Res Atmos 119(12):7382–7395. https://doi.org/10.1002/2013JD020560
Gu SY, Liu HL, Dou X, Li T (2016) Influence of the sudden stratospheric warming on quasi-2-day waves. Atmos Chem and Phys 16(8):4885–4896. https://doi.org/10.5194/acp-16-4885-2016
Harada Y, Hirooka T (2017) Extraordinary features of the planetary wave propagation during the boreal winter 2013/2014 and the zonal wave number two predominance. J Geophys Res Atmos 122(21):11374–11387. https://doi.org/10.1002/2017JD027053
Harada Y, Atsushi G, Hiroshi H, Fujikawa N (2010) A major stratospheric sudden warming event in January 2009. J Atmos Sci 67:2052–2069. https://doi.org/10.1175/2009JAS3320.1
Hirooka T, Hirota I (1985) Normal mode Rossby waves observed in the upper stratosphere Part II: Second antisymmetric and symmetric modes of zonal wavenumbers 1 and 2. J Atmos Sci 42(6):536–548
Hirooka (1986) Influence of normal mode Rossby Waves on the mean field: Interference with quasi-stationary waves. J Atmos Sci 43(19):2088–2097
Huang C, Zhang S, Chen G, Zhang S, Huang K (2017) Planetary wave characteristics in the lower atmosphere over Xianghe (117.00°E, 39.77°N), China, revealed by the Beijing MST radar and MERRA data. J Geophys Res Atmos 122(18):9745–9758. https://doi.org/10.1002/2017JD027029
Iida C, Hirooka T, Eguchi N (2014) Circulation changes in the stratosphere and mesosphere during the stratospheric sudden warming event in January 2009. J Geophys Res Atmos 119(12):7104–7115. https://doi.org/10.1002/2013JD021252
Iza M, Calvo N (2015) Role of stratospheric sudden warmings on the response to Central Pacific El Niño. Geophys Res Lett 42(7):2482–2489. https://doi.org/10.1002/2014GL062935
Kuttippurath J, Nikulin G (2012) A comparative study of the major sudden stratospheric warmings in the Arctic winters 2003/2004–2009/2010.

Atmos Chem Phys 12(17):8115–8129. https://doi.org/10.5194/acp-12-8115-2012
Lin B-D (1982) The behavior of winter stationary planetary waves forced by topography and diabatic heating. J Atmos Sci 39(6):1206–1226. https://doi.org/10.1175/1520-0469(1982)039%3c1206:TBOWSP%3e2.0.CO;2
Lu H, Pancheva D, Mukhtarov P, Cnossen I (2012) QBO modulation of traveling planetary waves during northern winter. J Geophys Res 117:D09104. https://doi.org/10.1029/2011JD016901
Luo Y, Manson AH, Meek CE, Meyer CK, Burrage MD, Fritts DC, Hall CM, Hocking WK, MacDougall J, Riggin DM, Vincent RA (2002) The 16-day planetary waves: multi-MF radar observations from the arctic to equator and comparisons with the HRDI measurements and the GSWM modelling results. Ann Geophys 20(5):691–709. https://doi.org/10.5194/angeo-20-691-2002
Madden RA (1978) Observations of large-scale travelling waves. Rev Geophys Space Phys 17(8):1935–1949. https://doi.org/10.1029/RG017i008p01935
Madden RA, Labitzke K (1981) A free Rossby wave in the troposphere and stratosphere during January 1979. J Geophys Res Oceans 86(C2):1247–1254. https://doi.org/10.1029/JC086iC02p01247
Manney GL, Kruger K, Sabutis JL, Sena SA, Pawson S (2005) The remarkable 2003–2004 winter and other recent warm winters in the Arctic stratosphere since the late 1990s. J Geophys Res 110:D04107. https://doi.org/10.1029/2004JD005367
Matsuno T (1971) A dynamical model of stratospheric sudden warming. J Atoms Sci 28(8):1479–1494. https://doi.org/10.1175/1520-0469(1971)028%3c1479:ADMOTS%3e2.0.CO;2
Matthewman NJ, Esler JG, Charlton-Perez AJ, Polvani LM (2009) A new look at stratospheric sudden warmings. Part III: polar vortex evolution and vertical structure. J Climate 22(6):1566–1585. https://doi.org/10.1175/2008JCLI2365.1
Matthias V, Hoffmann P, Rapp M, Baumgarten G (2012) Composite analysis of the temporal development of waves in the polar MLT region during stratospheric warmings. J Atmos Solar Terr Phys 90–91:86–96. https://doi.org/10.1016/j.jastp.2012.04.004
McDonald AJ, Hibbins RE, Jarvis MJ (2011) Properties of the quasi 16 day wave derived from EOS MLS observations. J Geophys Res 116:D06112. https://doi.org/10.1029/2010JD014719
Mitchell NJ, Middleton HR, Beard AG, Williams PJS, Muller HG (1999) The 16-day planetary wave in the mesosphere and lower thermosphere. Ann Geophys 17(11):1447–1456. https://doi.org/10.1007/s00585-999-1447-9
Pancheva D, Mukhtarov P, Mitchell NJ, Merzlyakov E, Smith AK, Andonov B, Murayama Y (2008) Planetary waves in coupling the stratosphere and mesosphere during the major stratospheric warming in 2003/2004. J Geophys Res Atmos 113:D12105. https://doi.org/10.1029/2007JD009011
Pancheva D, Mukhtarov P, Siskind DE (2018) The quasi-6-day waves in NOGAPS-ALPHA forecast model and their climatology in MLS/Aura measurements (2005–2014). J Atmos Solar Terr Phys 181:19–37. https://doi.org/10.1016/j.jastp.2018.10.008
Perlwitz J, Graf H-G (2001) Tropospheric-stratospheric dynamic coupling under strong and weak polar vortex conditions. Geophys Res Lett 28(2):271–274. https://doi.org/10.1029/2000GL012405
Pogoreltsev AI (2007) Generation of normal atmospheric modes by stratospheric vacillations. Izv Atmos Ocean Phys 43(4):423–435. https://doi.org/10.1134/S0001433807040044
Pogoreltsev AI, Kanukhina AY, Suvorova EV, Savenkova EN (2009) Variability of planetary waves as a signature of possibleclimatic changes. J Atmos Solar Terr Phys 71:1529–1539. https://doi.org/10.1016/j.jastp.2009.05.011
Rodas C, Pulido M (2017) A climatology of Rossby wave generation in the middle atmosphere of the Southern hemisphere from MERRA reanalysis. J Geophys Res Atmos 122(17):8982–8997. https://doi.org/10.1002/2017JD026597
Sakazaki T, Fujiwara M, Zhang X, Hagan ME, Forbes JM (2012) Diurnal tides from the troposphere to the lower mesosphere as deduced from TIMED/SABER satellite data and six global reanalysis data sets. J Geophys Res Atmos 117:D13108. https://doi.org/10.1029/2011JD017117
Salby ML (1981a) Rossby Normal Modes in Nonuniform Background Configurations. Part I: Simple Fields. J Atmos Sci 38(9):1803–1826. https://doi.org/10.1175/1520-0469(1981)038<1827:RNMINB>2.0.CO;2.
Salby ML (1981b) Rossby Normal Modes in Nonuniform Background Configurations. Part II. Equinox and Solstice Conditions. J Atmos Sci 38(9):1827–1840. https://doi.org/10.1175/1520-0469(1981)038<1827:RNMINB>2.0.CO;2
Salby ML (1984) Survey of planetary-scale traveling waves: the state of theory and observations. Rev Geophys 22(2):209–236. https://doi.org/10.1029/RG022i002p00209
Salby ML, Garcia RR (1987) Vacillations induced by interference of stationary and traveling planetary waves. J Atmos Sci 44(19):2679–2711. https://doi.org/10.1175/1520-0469(1987)044%3c2679:VIBIOS%3e2.0.CO;2
Schroeder S, Preusse P, Ern M, Riese M (2009) Gravity waves resolved in ECMWF and measured by SABER. Geophys Res Lett 36:L10805. https://doi.org/10.1029/2008GL037054
Scott RK, Polvani LM (2006) Internal variability of the winter stratosphere. Part I: time-independent forcing. J Atmos Sci 63(11):2758–2776. https://doi.org/10.1175/JAS3797.1
Seppälä A, Lu H, Clilverd MA, Rodger CJ (2013) Geomagnetic activity signatures in wintertime stratosphere wind, temperature, and wave response. J Geophys Res Atmos 118(5):2169–2183. https://doi.org/10.1002/jgrd.50236
Škerlak B, Sprenger M, Wernli H (2014) A global climatology of stratosphere–troposphere exchange using the ERA-Interim data set from 1979 to 2011. Atmos Chem Phys 14(2):913–937. https://doi.org/10.5194/acp-14-913-2014
Tomikawa Y, Sato K, Watanabe S, Kawatani Y, Miyazaki K, Takahashi M (2012) Growth of planetary waves and the formation of an elevated stratopause after a major stratospheric sudden warming in a T213L256 GCM. J Geophys Res 117:D16101. https://doi.org/10.1029/2011JD017243
Vincent RA (1990) Planetary and gravity waves in the mesosphere and lower thermosphere. Adv Space Res 10(12):93–101. https://doi.org/10.1016/0273-1177(90)90388-G
Vineeth C, Pant TK, Kumar KK, Sumod SG (2010) Tropical connection to the polar stratospheric sudden warming through quasi 16-day planetary wave. Ann Geophys 28(11):2007–2013. https://doi.org/10.5194/angeo-28-2007-2010
Wu DL, Hays PB, Skinner WR, Marshall AR, Burrage MD, Lieberman R, Ortland DA (1993) Observations of the quasi 2-day wave from the High Resolution Doppler Imager on Uars. Geophys Res Lett 20(24):2853–2856. https://doi.org/10.1029/93GL03008
Wu DL, Hays PB, Skinner WR (1994) Observations of the 5-day wave in the mesosphere and lower thermosphere. Geophys Res Lett 21(24):2733–2736. https://doi.org/10.1029/94GL02660
Xiong J, Wan W, Ding F, Liu L, Hu L, Yan C (2018) Two day wave traveling westward with wave number 1 during the sudden stratospheric warming in January 2017. J Geophys Research Space Phys 123(4):3005–3013. https://doi.org/10.1002/2017JA025171

Publisher's Note